Research Article/Systems and Computer Engineering http://doi.org/10.15446/ing.investig.106558

Development and Validation of a Dry Electrode Array for sEMG Recording and Hand Movement Recognition

Desarrollo y validación de un arreglo de electrodos secos para la adquisición de señales sEMG y el reconocimiento de los movimientos de la mano

Cinthya L. Toledo-Peral[1], Ana I. Martín-Vignon-Whaley[2], Jorge A. Mercado-Gutiérrez[3], Arturo Vera-Hernández[4], Lorenzo Leija-Salas[5], and Josefina Gutiérrez-Martínez[6]

ABSTRACT

Surface electromyography (sEMG) signals are an indirect measurement of muscle activity, and their applications range from biomechanics to control and rehabilitation. Hand movement recognition is a very difficult endeavor due to forearm anatomy. Hence, a multichannel approach for signal acquisition and processing is required. Conventional electrodes can limit the ease-of-use and repeatability of multi-channel sEMG recordings. New techniques have been proposed in this regard, with dry electrodes being one of them. Dry electrode technology has enabled the design of better donning and doffing procedures for multichannel sEMG recording, particularly for rehabilitation and prosthetic applications. However, there is a debate about the quality of the signals recorded with them and their usefulness for the recognition of multiple hand movements. To mitigate these quality issues, this work proposes an array of reusable stainless steel dry electrodes for multichannel sEMG recording with a design that facilitates its positioning on the forearm. The dry electrodes were characterized through electrical impedance measures and a Bland-Altman test. They were found to have similar characteristics to standard, disposable sEMG pre-gelled electrodes. For placement repeatability and application feasibility, an anatomy-based electrode positioning protocol was implemented with 17 healthy subjects and six hand movements. To evaluate the application feasibility of the electrode array, a feed-forward artificial neural network was trained to classify signals from the six movements, with a 97,86±0,58% accuracy. The amplitude of the sEMG signals for two antagonist movements was compared, finding a 24,81% variation. The dry electrode array showed feasibility in acquiring and classifying sEMG signals of hand movements with high accuracy.

Keywords: dry electrodes, Bland-Altman, anatomical positioning array, hand movement classification

RESUMEN

Las señales de electromiografía de superficie (sEMG) son una medida indirecta de la actividad muscular, y sus aplicaciones van desde biomecánica hasta control y rehabilitación. La identificación de movimientos de la mano es una tarea muy complicada debido a la anatomía del antebrazo, por lo que se requiere un enfoque multicanal para adquisición y procesamiento de señales. Los electrodos convencionales pueden limitar la facilidad de uso y la repetibilidad de los registros sEMG multicanal. Se han propuesto nuevas técnicas para ello, entre ellas los electrodos secos. La tecnología de electrodos secos ha permitido el diseño de mejores procedimientos de colocación y remoción para registro sEMG multicanal, particularmente en aplicaciones de rehabilitación y prótesis. Sin embargo, existe un debate sobre la calidad de las señales registradas con ellos y su utilidad para el reconocimiento de múltiples movimientos de la mano. Para mitigar estos problemas de calidad, se propone un arreglo de electrodos secos reutilizables de acero inoxidable para registro sEMG multicanal con un diseño que facilita su posicionamiento en el antebrazo. Estos electrodos se caracterizaron mediante mediciones de impedancia eléctrica y una prueba Bland-Altman. Se encontró que tienen características similares a los electrodos pregelados desechables estándar para sEMG. Para la repetibilidad de la colocación y su viabilidad de aplicación, se implementó un protocolo de colocación de electrodos basado en la anatomía con 17 sujetos sanos y seis movimientos

[1] Bachelor's in Electronics, Benemérita Universidad Autónoma de Puebla, Mexico. MSc in Electrical Engineer in Bioelectronics, Centro de Investigación y Estudios Avanzados del Instituto Politécnico Nacional, Mexico. Affiliation: Research Biomedical Engineer, Instituto Nacional de Rehabilitación Luis Guillermo Ibarra Ibarra, Mexico, and PhD Student in Electrical Engineer – Bioelectronics, Centro de Investigación y Estudios Avanzados del Instituto Politécnico Nacional, Mexico. Email: phd.toledo@outlook.com

[2] Bachelor's in biomedical engineering, Universidad La Salle, Mexico. E-mail: anaimvw@gmail.com

[3] Bachelor in Electronics, Benemérita Universidad Autónoma de Puebla, Mexico. MSc in Biomedical Engineering, Universidad Autónoma Metropolitana, Mexico. PhD in Electrical Engineering, Bioelectronics, Centro de Investigación y Estudios Avanzados del Instituto Politécnico Nacional, Mexico. Affiliation: Medical science researcher, Instituto Nacional de Rehabilitación Luis Guillermo Ibarra Ibarra, Mexico. E-mail: jorgea.mercadog@gmail.com

[4] Biomedical engineer, Instituto Politécnico Nacional, Mexico. MSc in Electrical Engineering, Bioelectronics, Centro de Investigación y Estudios Avanzados del Instituto Politécnico Nacional, Mexico. PhD in Engineering, Institut Polytechinique de Lorraine, France. Affiliation: Researcher 3C, Centro de Investigación y Estudios Avanzados del Instituto Politécnico Nacional, Mexico. E-mail: arvera@cinvestav.mx

[5] Industrial engineer, Instituto Tecnológico de San Luis Potosí, Mexico. MSc in Electrical Engineering, Bioelectronics, Centro de Investigación y Estudios Avanzados del Instituto Politécnico Nacional, Mexico. PhD in Engineering, Université de Nancy, France. Affiliation: Researcher 3D, Centro de Investigación y Estudios Avanzados del Instituto Politécnico Nacional, Mexico. E-mail: lleija@cinvestav.mx

[6] Bachelor's in biomedical engineering, Universidad Iberoamericana, Mexico. MSc in Electrical Engineering, Bioelectronics, Centro de Investigación y Estudios Avanzados del Instituto Politécnico Nacional, Mexico. PhD in Engineering, Universidad Nacional Autónoma de México. Affiliation: Head of the medical engineering research division, Instituto Nacional de Rehabilitación Luis Guillermo Ibarra Ibarra, Mexico. E-mail: josefina_gutierrez@hotmail.com

de la mano. Finalmente se entrenó una red neuronal artificial prealimentada para clasificar señales de los seis movimientos, con una precisión del 97,86±0,58 %. Se comparó la amplitud de las señales sEMG para dos movimientos antagonistas, encontrando una variación del 24,81 %. El arreglo de electrodos secos mostró viabilidad para adquirir y clasificar registros sEMG de los movimientos de la mano con gran precisión.

Palabras clave: electrodos secos, Bland-Altman, arreglo de posicionamiento anatómico, clasificación de movimientos de la mano

Received: December 28th, 2022
Accepted: July 18th, 2023

Introduction

Hand movements are complex to perform, acquire, and emulate. Many structures are involved in hand movements, especially forearm muscles. In order to analyze them, they can be divided into three regions: anterior, posterior, and external. The anterior region has several muscles divided into four planes that include the round pronator and anterior ulnar, the superficial common long flexor of the fingers, the flexor of the thumb and deep common flexor of the fingers, and the pronator square. The external region is composed of the long supinator, the first external radial, the second external radial, and the short supinator. Finally, the posterior region holds the flexor muscles, among others (Hall, 2011). Around half of these muscles are deep enough to be challenging to access from the surface of the skin (Mitchell and Whited, 2019), and most of them are either layered or braided with adjacent muscles. Moreover, from a bio-signal acquisition perspective, it is difficult to place enough electrodes in a such small area to match muscle anatomy and acquire signals, thus allowing to distinguish between hand movements.

Muscle fibers contract while being controlled by electrical signals that are transmitted through the nervous system and generated by units called *motor neurons*. These electrical signals are recorded on the surface of the skin, which is known as *surface electromyography* (sEMG). To record and interpret these signals, bipolar electrodes are placed at the belly of the muscle where the transversal area of the motor units is larger. This position is optimal for obtaining the highest amplitude signal, which also contains more information on muscle contraction. According to the recommendations provided by *The Surface Electromyography for the Non-Invasive Assessment of Muscles* (SENIAM) and the *Consensus for Experimental Design in Electromyography* (CEDE) projects, passive bipolar electrodes should have a separation of approximately 2,5 cm, the electrodes should be aligned relative to the fascicle direction, a reference should be placed at a dielectric site, and there has to be a contact area on the skin of at least 10 mm in diameter (Besomi *et al.*, 2019; Biga *et al.*, n.d.; Hermens *et al.*, 2000; Merletti and Farina, 2016; "Recommendations for the Practice of Clinical Neurophysiology: Guidelines of the International Federation of Clinical Neurophysiology", 1999).

In most cases, an sEMG signal from one muscle does not yield enough information, so the use of several acquisition channels has become common practice. Nevertheless, the number of channels needed for different applications varies depending on the aim and purpose (Kapelner *et al.*, 2016; Liu, 2015; Peng *et al.*, 2016).

For some applications (*e.g.*, a therapy session), placing more than two or three pairs of electrodes can be time-consuming. Moreover, placing too many electrodes in a limited time span could rush the process and lead to mistakes and variability. The use of disposable electrodes also represents higher costs and waste.

Commercially available acquisition systems come with pre-gelled electrodes that are ready to use, but most applications require placement in muscle targets, allowing for only minimal variations (Al-Ayyad *et al.*, 2023). When going through the literature, one may notice that the clinical applications of wearable devices tend to be unified to match conventional therapy, which is the gold standard. These systems may benefit from a ready-to-wear electrode array, useful for repetitive measurements.

Another example that requires the placement of many electrodes corresponds to prosthetic control applications, such as upper limb prostheses based on pattern recognition techniques, which may include up to eight pairs of electrodes to focus on biceps and forearm muscles. Most of these applications do not use arrays but personalized positioning (Liu, 2015; Phinyomark *et al.*, 2014). The Myo armband is an acquisition system embedded in an eight-channel geometrical dry electrode array. All channels are equidistantly placed around the forearm in the proximal region. This armband also has a three-axes gyroscope, a three-axes accelerometer, a three-axes magnetometer, and a Bluetooth module (Myo Armband, Thalmic Labs Inc.) (Visconti *et al.*, 2018). Other systems designed for upper limb sEMG signal acquisition that use dry electrodes include those from Biometrics Ltd. (Newport, UK) and the silver electrodes of Trigno Avanti (Delsys Inc., Massachusetts, USA) (Al-Ayyad *et al.*, 2023).

The electrode arrays found in the literature have a geometrical matrix design, and the signals acquired can be treated as one-dimensional vectors, 2D images, or 3D heat maps (Barbero *et al.*, 2012b; Dai *et al.*, 2019; Guzmán *et al.*, 2011; Moin *et al.*, 2018; Peng *et al.*, 2016; Reategui and Callupe, 2017; Rojas-Martínez *et al.*, 2013; Rui Ma *et al.*, 2010; Ruvalcaba *et al.*, 2017; Topalović *et al.*, 2019). These types of arrays are advantageous when one desires to acquire a larger number of channels, and they are mainly used to evaluate areas of muscle contribution during upper limb isometric contractions. In some cases, subjects arms are constrained to avoid undesired movements (Dai *et al.*, 2019; Moin *et al.*, 2018; Peng *et al.*, 2016; Rojas-Martínez *et al.*, 2013; Topalović *et al.*, 2019; Urbanek and van der Smagt, 2016). Furthermore, geometrical matrices do not require previous knowledge of the site's anatomy or customization for

placement on each patient. Still, they are not recommended for evaluating movements (isotonic contraction) where the transient part of the signal is relevant; the subject must be able to move as normally as possible. Almost all arrays found in the literature say they use dry electrodes, but several have been found to need conductive gel to properly function (Dai *et al*., 2019; Guzmán *et al*., 2011; Peng *et al*., 2016; Rodrigues *et al*., 2020; Rojas-Martínez *et al*., 2013; Topalović *et al*., 2019; Urbanek and van der Smagt, 2016).

The only type of pre-positioned dry electrodes for sEMG signal acquisition is used in myoelectric prosthesis, where movements are activated through direct control, generally using two acquisition channels placed in antagonist muscles. In addition, the electrodes are normally integrated into the socket of the prosthesis (three electrodes: two larger bipolar ones and a small one for the reference in the middle), so they are used in large muscles, *e.g.*, the biceps and triceps, where electrodes can withstand a 2 cm location shift without considerable differences in the outcome signal (Losier *et al*., 2011; Young *et al*., 2011).

Dry electrodes play an essential role in the repeated usability of positioning electrode arrays. As a main advantage, dry electrodes do not need conductive electrolyte gel to function correctly; the user just needs to wait for a period of 10 to 15 min before recording a signal (Meziane *et al*., 2013), which falls within the preparation time for an sEMG recording session. Another benefit is that they do not need intensive skin cleaning, are reusable (thus reducing medical waste), and have long-term use applications, unlike gelled electrodes that dry out over time (Srinivasa and Pandian, 2017).

Dry electrodes are built using different materials, such as stainless steel, conductive textiles, and flexible polymers. They are used in research and are commercially available (Xie *et al*., 2013; Niu *et al*., 2021). The SENIAM and CEDE projects recommend metal materials such as stainless steel, platinum, and Ag/AgCl for building dry electrodes (Besomi *et al*., 2019; Hermens *et al*., 2000).

Moreover, there is a small recurrent set of materials used to fabricate dry electrodes and electrode arrays. Textile electrodes are widely used, but they are not suitable for dry applications in small areas (Ruvalcaba *et al*., 2017; Vojtech *et al*., 2013) because they have a higher sensibility to motion and pressure, which can lead to higher skin-contact impedance and noisy signals (Chi *et al*., 2010; Xie *et al*., 2013; Meziane *et al*., 2013; Puurtinen *et al*., 2006; Srinivasa and Pandian, 2017). In Kusche *et al*. (2019), five materials (gold, stainless-steel, rubber with/without texture, and textile) are compared when used for dry electrode fabrication and against Ag/AgCl gelled electrodes. Regarding frequency response, dry electrodes show lower impedance values. After 15 min of contact with the skin, the impedance of stainless-steel electrodes stabilizes and maintains its value for up to 30 min. Of the six materials, stainless-steel has a higher impedance than gold and Ag/AgCl, albeit lower than that of the other materials.

Some metallic options have been tested for sEMG signal acquisition, such as brass dry electrodes (Ruvalcaba *et al*., 2016) under 10 mm in diameter which yield impedance values like those of pre-gelled commercial electrodes (Ghoshdastider *et al*., 2012; Vojtech *et al*., 2013). Nevertheless, stainless-steel electrodes have two main advantages: they have a simple manufacturing process, and they can be reused because of their corrosion resistance (Albulbul, 2016; Gan *et al*., 2019). Therefore, this material is a good option for manufacturing small surface electrodes, wherein contact issues will not be a concern (Guo *et al*., 2020).

Stainless steel electrodes perform as well as commercial dry electrodes, and their manufacturing process is simple ("Recommendations for the Practice of Clinical Neurophysiology: Guidelines of the International Federation of Clinical Neurophysiology", 1999). Stainless steel electrodes are antibacterial, do not rust, and can be used for long-term measures. Furthermore, stainless steel is among the metals less likely to cause an allergic skin reaction, and they are recommended by the SENIAM (Hermens *et al*., 2000).

Even though there are different proposals regarding materials, configurations, and embedded acquisition systems, to the best of our knowledge, and after a thorough literature analysis, there is no evidence of anatomical positioning arrays using dry electrodes for sEMG signal acquisition (Palumbo *et al*., 2021).

To be able to simultaneously acquire sEMG signals from several muscles and easily find the best location for multiple electrodes within the forearm, in order to record the patterns of hand movements, this work proposes an array of 17 dry electrodes positioned on anatomical sites at the forearm, which are fixed using a textile sleeve with a design based on anthropometric measures. This design allows recording eight sEMG channels from the forearm muscles at their correct anatomical sites. We hypothesize that assessing the functionality of the forearm dry electrode anatomical array for the acquisition of sEMG signals regarding six movements (rest, hand opening, power grasp, fine pinch, supination, and pronation) will result in the acquisition of usable signals for pattern recognition.

Methodology

A total of 22 abled-body volunteers participated in two types of evaluations. 17 subjects participated in anthropometrical measurements, and five subjects participated in signal acquisition for the digital processing of the data. All subjects signed an informed consent. The procedures carried out in this work were aimed at performing a proof-of-concept to evaluate the functionality of an array of dry electrodes with anatomy-based positioning. All procedures were approved by the Institutional Research and Ethics Boards, as part of protocol No. 38/16.

To design a dry electrode array for sEMG signal acquisition based on anatomical positioning, the first step was to locate the muscles of interest in the forearm, which is a small area with multiple muscles, most of them narrow and short. For each hand movement, there is a set of known muscles involved (Barbero *et al*., 2012a; Hall, 2011). These can be seen in Table 1.

Table 1. Muscles involved in the target hand movements

Movement	Muscles Involved
Open Hand	Finger extensors, fifth finger extensor, index extensor, long extensor of the thumb, short extensor of the thumb, long abductor of the thumb
Power Grasp	Long palmar, superficial flexor of the fingers, deep flexor of the fingers of the hand, long flexor of the thumb, brachioradialis
Fine Pinch	Long palmar, superficial flexor of the fingers, long flexor of the thumb, brachioradialis
Supination	Long supinator, short supinator
Pronation	Pronator square, pronator teres

Source: Barbero *et al*. (2012a); Hall (2011b)

Regarding the first evaluation, 17 volunteer abled-body subjects participated in the protocol for the anatomical positioning of electrodes (eight females 22,8 ± 3,14 years of age, with a height of 1,72 ± 16,2 m and a weight of 72,12 ± 16,20 kg; and nine males 23 ± 3,1 years of age, with a height of 1,73 ± 0,12 m and a weight of 71,75 ± 16,10 kg). To trace the best position at the forearm for sEMG signal acquisition, eight muscle sites were located by identifying the insertions of the tendons and the ventral part of the muscles of interest. Then, the subjects were asked to perform five repetitions of six hand movements, *i.e.*, hand opening, power grasp, fine pinch, supination, pronation, and rest, while the muscles were palpated.

Afterwards, the position for the bipolar acquisition channel was marked, centered on top of the ventral area of the muscles of interest, with a separation of 2,5 cm. This process started at the brachioradialis muscle and was repeated towards the lateral region of the forearm (externally). A personalized map of the anatomical positioning of sEMG electrodes was obtained for each subject, which was then transferred to an acetate sheet to create *individual templates*. The initial marks for the electrodes were positioned in the brachioradialis, so this muscle was used as a common point to overlap the *individual templates*. The resulting positions were used to propose the *general template* of the anatomical positioning array (APA). These steps are exemplified in Figure 1.

The design of a set of dry electrodes was proposed and carried out. To place the dry electrodes, a textile sleeve design was developed, which was based on the anthropometric measures of the participants, as follows:

- Wrist circumference
- Length between the elbow and the wrist
- Half of the elbow-wrist length
- Half of the half of the elbow-wrist length
- Forearm circumference at the half of the half of the elbow-wrist length

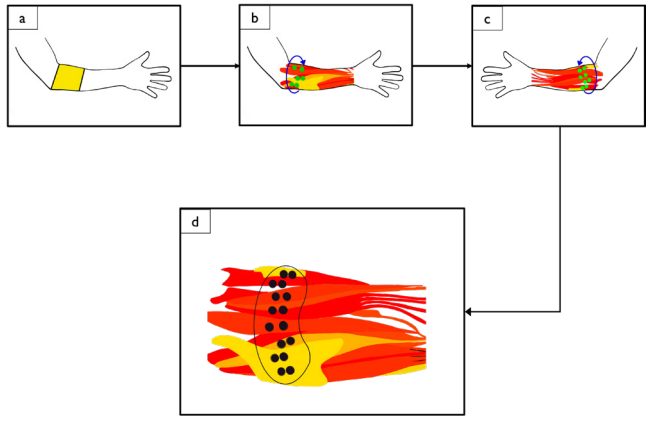

Figure 1. Schematic model of the protocol to map the anatomical sites for electrode positioning. a) Approximate area where the ventral site of the target muscles at the forearm are located. b) Location of the ventral zone of the forearm muscles from the lateral view. c) Location of the ventral zone of muscles from the medial view. d) Forearm template with the location of eight main sites of muscle activation during hand movements. This diagram is an unfolded representation of the muscles found in both lateral and medial views.
Source: Authors

In essence, the forearm length was divided in four segments: proximal, medial-proximal, medial-distal, and distal. The forearm circumference was measured at the boundary between the proximal and medial proximal segments. The latter site concurs with the area of the forearm where most electrodes are located in the *general template*. This area is shown in Figure 1a.

A common reference dry electrode was placed at the olecranon (a dielectric site) using a piece of elastic fabric that is separated from the textile sleeve. The fabric used to manufacture the sleeve was made of 92% polyester and 8% elastane, and it can withstand a temperature of 160 °C.

The APA was mounted on a textile sleeve to be placed over the forearm in order to acquire eight bipolar channels of sEMG signals from hand movements. This **F**orearm dry **EL**ec**T**rodes anatomical array was named FELT, an evolution from a first array proposed in Toledo-Peral *et al*. (2018).

The designed dry electrodes and the positioning array were subjected to the following functional evaluations:

- Dry electrodes evaluation 1: electrode-skin electrical impedance characterization
- Dry electrodes evaluation 2: Bland-Altman agreement assessment
- FELT functionality evaluation 1: anatomical array
- FELT functionality evaluation 2: signal acquisition and data processing

Dry electrodes design and manufacture

The electrodes were designed using CAD software (Dassault Systèmes SolidWorks Corporation, USA) and manufactured in a Computer Numeric Control (CNC) machine. The electrode was lathed as one piece using a ½ inch 304 stainless steel bar. It was designed to be 12 mm in diameter. On one side, the area for skin contact was flat and polished, and, on the other side, it had a 10 mm thread to connect the lead cable. An acorn nut was placed on the thread of the electrode to fix it to the sleeve and the connection cable.

Dry electrodes evaluations

The evaluations performed on the designed dry electrodes (sEMG-DRY) were electrode-skin impedance characterization and a Bland-Altman agreement assessment. To compare the electrodes against the standard reference, pre-gelled standard commercial disposable electrodes (sEMG-GEL) were used (Kendall, COVIDIEN).

Dry electrodes evaluation 1: electrode-skin electrical impedance characterization

According to Martin *et al*. (2018), the circuit used for impedance measurements was powered by an 8 Vpp sinusoidal signal provided by a function generator (AFG320, Sony Tektronix), which acted as a power supply. It was connected in series with a 100 kΩ resistor, and then to an electrode in contact with the skin. The second electrode in contact with the skin was connected to a 100 Ω resistor and then to the generator ground.

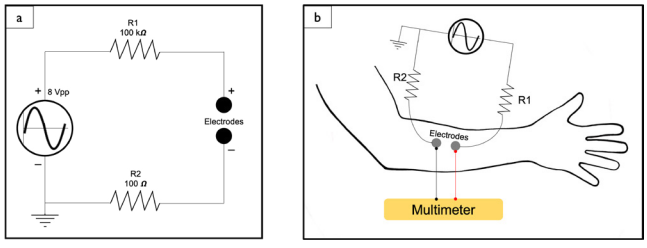

Figure 2. Measurements at the skin-dry electrode interface. a) Electronic circuit used to power the dry electrodes. b) Configuration used to measure the resulting electrode-skin impedance
Source: Authors

The sEMG-DRY electrodes were placed and left to settle for 15 min before any signals were acquired. The electrical impedance response of the electrode was measured for a frequency range between 20 and 500 Hz, with a frequency sweep and increments of 20 Hz (20-100 and 400-500 Hz) and 50 Hz (100-400 Hz). The peak-to-peak voltage variations were measured with a multimeter (FLUKE, model 189). The electric current was calculated through Equation (1), and the electrical impedance values were calculated with Equation (2) (Martin *et al*., 2018):

$$I = \frac{V_{ab}}{R_1} \tag{1}$$

$$Z = \frac{V_{bc}}{I} \tag{2}$$

where I is the current; V_{ab} is the measured voltage that passes through R_1, which has a resistance of 100 kΩ; V_{bc} denotes the measured voltage that passes through the electrodes characterized; and Z represents the calculated electrical impedance, which was measured for each frequency and repeated for 10 sessions with a 23-year-old female abled-body subject for both the sEMG-DRY and the sEMG-GEL electrodes.

Dry electrodes evaluation 2: Bland-Altman agreement assessment

The Bland-Altman test was used to assess the agreement between the signals acquired by the sEMG-DRY and the sEMG-GEL electrodes. The first step was to choose the parameter to be extracted in order to perform the evaluation. In this case, we selected the mean temporal amplitude and calculated it using the area under the curve A of the signal for the period N regarding the signals obtained with the electrodes. This was calculated using Equation (3).

$$A = \int_0^N f(t)\,dt \tag{3}$$

where $f(t)$ is the signal of interest for a length N.

The Bland-Altman or difference plot is a statistical graphical method used to analyze the agreement between the measurements of two instruments, or, in this case, the acquired sEMG signals using two types of electrodes. This plot compares the sEMG-DRY signals (new measurement technique) against the sEMG-GEL ones (the reference/gold standard). This plot helps to assess the magnitude of disagreement (or bias) and determine if there is any trend. It is expected that, if the differences are normally distributed (Gaussian), 95% of them will lie between the limits of agreement (mean of differences ± 1,96 standard deviation, or SD). Therefore, if the bias (as estimated by the mean difference and the SD of the differences) is small, the two methods can be used interchangeably, and the new technique can replace the established one.

The precision of the estimates was determined by calculating the limits of agreement, the standard error of the mean (SEM), and the standard error of the limits of agreement (SELA). These limits were calculated using Equations (4) and (5), respectively.

$$SEM = \sqrt{SD^2 / n} \tag{4}$$

$$SELA = \sqrt{3 \cdot SD^2 / n} \tag{5}$$

where n is the sample size, and SD denotes the standard deviation of the differences.

A 95% confidence interval (CI) was calculated for the bias, as well as for the lower limit (LL) of agreement and for the upper limit (UL) of agreement. These values were calculated using Equations (6), (7), and (8), respectively.

$$CI\left(95\%\right) = -\bar{d} \pm \left(t \cdot SEM\right) \tag{6}$$

$$CI\left(95\%\right)LL = -LL \pm \left(t \cdot SELA\right) \tag{7}$$

$$CI\left(95\%\right)UL = -UL \pm \left(t \cdot SELA\right) \tag{8}$$

where $\bar{d}$ is the mean difference or bias of the measurements obtained from the sEMG-DRY and the sEMG-GEL electrodes, and t takes a value of 2,0010 (Bland and Altman, 1986).

The sEMG signals of four 20 to 22 years old abled-body female subjects who performed power grasp isotonic contractions using both types of electrodes were acquired for the Bland-Altman agreement assessment. These signals were recorded at the brachioradialis muscle of the right arm (dominant side). Three repetitions lasting 3 s were performed, with 10 s rest. The acquired signals were divided into 0,5 s segments for the statistical analysis, which is also the window length selected for the processing algorithm. In our experience, the first 3 s of the contraction contain the transient information of the hand movement. We found no need to record or use the posterior stationary segment; the 10 s of rest ensure that the subject has enough time to relax their muscles and prepare for the next repetition (Toledo *et al*., 2018).

FELT functionality evaluation 1: anatomical array

The FELT was used to acquire sEMG signals from one 35-year-old abled-body male. FELT placement was performed following the *FELT positioning protocol* described below. This is shown in Figure 3.

1. Place the forearm in supine position
2. Place the FELT next to it with the seams looking upwards
3. Slide the hand through the FELT, maintaining the position for sections of the FELT (upper and lower)
4. Align the seams of the FELT with the line formed by the middle point of the flexor retinaculum and the ulnar fossa
5. Verify that the FELT has a tight fit over the forearm
6. Remove the bottom of the FELT
7. Place the reference electrode on the olecranon using a piece of elastic fabric

The electrodes placed in contact with the skin were left to settle for 15 min before any signals were acquired.

FELT functionality evaluation 2: signal acquisition and data processing

sEMG signals were acquired with the amplifier Shimmer3 EMG unit (Shimmer), connected via Bluetooth, at a 1 024 Hz sampling frequency, a fixed gain of 12 for the amplifier, and a bipolar configuration for eight channels. Signal processing was performed using MATLAB 2021b. For this evaluation, a 34-years-old abled-body male volunteer underwent five sessions of sEMG signal acquisition using the FELT.

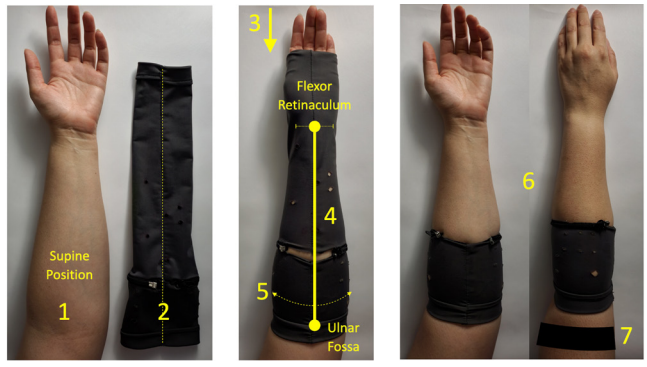

Figure 3. Positioning protocol for the FELT. The numbers match the steps designed to ensure a proper anatomical placement.
Source: Authors

In the case of the sEMG-GEL electrodes, the skin had to be previously cleaned to improve contact and for the adhesive to hold on longer. Then, the electrodes were positioned using the *general template*, and the reference electrode was placed at the olecranon.

An sEMG signal acquisition protocol was implemented, and five trials were performed, each one consisting of three contractions with a 3 s duration and 10 s rests. The algorithm acquired the sEMG signal using Shimmer3 and sent it directly to MATLAB. The hand movement protocol is shown in Figure 4.

Offline processing was performed based on a previously developed algorithm (Toledo-Peral *et al*., 2018), with a few adjustments since a different acquisition system was being used. A time-frequency approach using the discrete wavelet transform (DWT) discriminated the signal content from artefacts and components not in the range of the frequencies of interest.

For either algorithm, the signal went through a Notch filter to eliminate the 60 Hz line interference. Then, a Daubechies wavelet 'db9' eight-level decomposition was performed for baseline elimination. Later, a wavelet Daubechies 'db4' two-level decomposition was performed to obtain the frequency range of interest for the sEMG components. The absolute value of the signal was calculated to finally go through a wavelet Haar nine-level decomposition to find the envelope. Using the last signal, a threshold was established to segment the active portion of the sEMG

signals. This is depicted in Figure 5. From the segmented signal, several parameters were calculated. The parameters calculated using Equations (9) to (15) (Phinyomark *et al.*, 2013) are shown in Table 2.

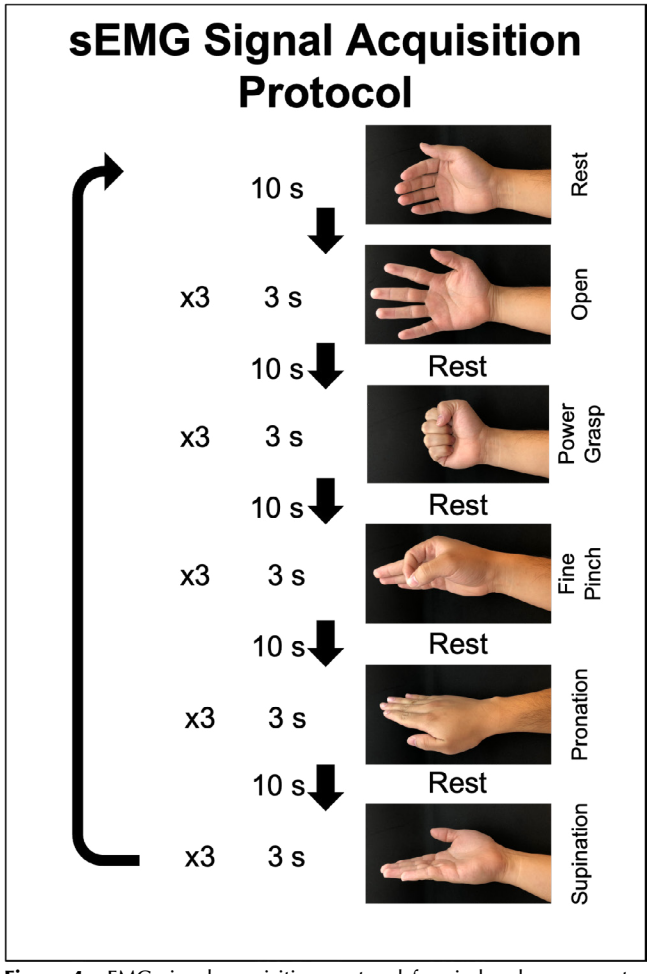

Figure 4. sEMG signal acquisition protocol for six hand movements. Each movement was performed three times for 3 s, with 10 s rest between movements.
Source: Authors

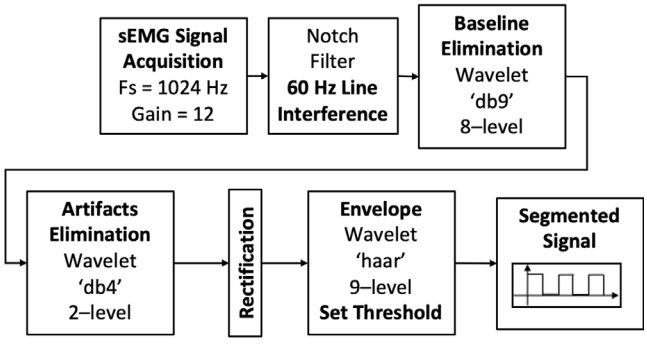

Figure 5. Signal processing algorithm based on DWT decomposition. This algorithm was used for signals acquired with either sEMG-DRY or sEMG-GEL electrodes.
Source: Authors

Table 2. Equations for seven features that characterize sEMG signals

Feature	Equation	Equation Number
Mean absolute value	$MAV = \frac{1}{n}\sum_{i=1}^{n}\lvert x_i\rvert$	(9)
Integral of the absolute value	$IAV = \sum_{i=1}^{n} x_i$	(10)
Root mean square	$RMS = \sqrt{\frac{1}{n}\sum_{i=1}^{n}(x_i)^2}$	(11)
Variance	$V = \frac{1}{n-1}\sum_{i=1}^{n}(x_i-\bar{x})^2$	(12)
Skewness	$s = \frac{\frac{1}{n}\sum_{i=1}^{n}(x_i-\bar{x})^3}{\left(\sqrt{\frac{1}{n}\sum_{i=1}^{n}(x_i-\bar{x})^2}\right)^3}$	(13)
Slope signal change	$SSC = \begin{cases} 1 & x_i > x_{i+1} \;\&\; x_i > x_{i-1} \\ 1 & x_i < x_{i+1} \;\&\; x_i < x_{i-1} \\ 0 & else \end{cases}$	(14)
Wave-length	$WL = \sum_{i=1}^{n}\lvert x_i - x_{i-1}\rvert$	(15)

Source: Phinyomark *et al.* (2013)

Here, x denotes the sEMG signal, x_i is a sample of the signal, $\bar{x}$ represents the mean of x, σ is the standard deviation, and n denotes the length of the signal.

For each of the six hand movements, the seven parameters (Phinyomark *et al.*, 2013) were calculated and fed to an Artificial Neural Network (ANN).

Results and Discussion

The functionality of the proposed dry electrode APA for sEMG signal acquisition at the forearm while performing six hand movements is evaluated in this section. The 17 sEMG-DRY electrodes are composed of flat, round, stainless steel cylindrical pieces, each 12 mm in diameter, with a threaded section used to affix them to the textile sleeve and the connection cable using an acorn nut. Compared to previous designed prototypes (Martin *et al.*, 2018; Toledo-Peral *et al.*, 2018), this one yields a signal with fewer noise artefacts such as line interference. The contact area of the sEMG-DRY electrode ensured uniform contact with the skin. All electrodes were identically built.

Then, the designed sEMG-DRY electrodes were evaluated regarding electrode-skin electrical impedance and compared to the sEMG-GEL ones using the Bland-Altman agreement assessment test.

Dry electrodes evaluation 1: electrode-skin electrical impedance characterization

The electrode-skin electrical impedance (mean ± standard deviation) was measured for a frequency range of 20 to 550 Hz for both the sEMG-DRY and the sEMG-GEL electrodes. The corresponding electrical impedance plots are shown in Figure 6. The electrical impedance response had a similar behavior in both electrode types regarding the attenuation of their amplitude along the frequency range. The impedance values were higher for lower frequencies in sEMG-DRY electrodes. The literature states that dry electrodes have higher impedance values than pre-gelled standard electrodes (Garcia *et al*., 2007; Xie *et al*., 2013).

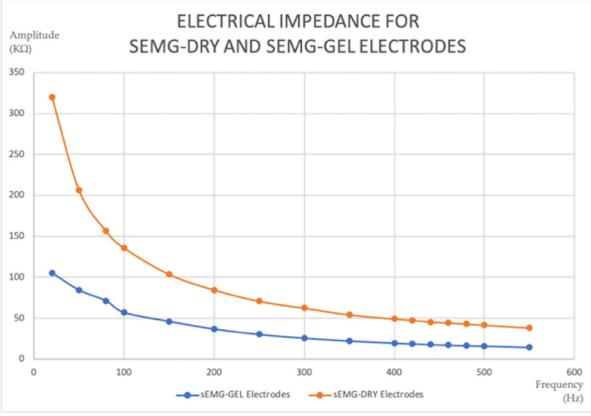

Figure 6. Electrical impedance response for a frequency range of 20 to 550 Hz for both sEMG-DRY and sEMG-GEL electrodes
Source: Authors

sEMG-DRY electrodes have some advantages over sEMG-GEL ones. Firstly, their placement is faster. Over time, the conductive gel degrades and dries, yielding low quality signals, while sEMG-DRY electrodes have improved contact because they take advantage of the properties of the skin. sEMG-DRY electrodes allow for long-term measurements, can be reused endless times with proper care, do not generate waste, are antibacterial, and pose a lower risk of skin rashes (Srinivasa and Pandian, 2017).

Dry electrodes evaluation 2: Bland-Altman agreement assessment

To assess whether the measurements provided by a new instrument are valid, they must be compared with those obtained via a gold standard instrument. To this effect, a Bland-Altman agreement assessment was performed. We wanted to know if sEMG-DRY electrodes could be used as sEMG-GEL ones, so we acquired sEMG signals using both types from four abled-body female volunteers. The parameter chosen for the test was the mean temporal amplitude, and a total 60 records of sEMG signals were involved in the calculations. The data were obtained using Equation (3) and are shown in Table 3. The Bland-Altman plot is shown in Figure 7.

Table 3. Mean temporal amplitude (*A*) of sEMG signals acquired using sEMG-DRY and sEMG-GEL electrodes

Reps	sEMG–DRY Electrodes Mean temporal amplitude [mV]				sEMG–GEL Electrodes Mean temporal amplitude [mV]			
	Subject				*Subject*			
	1	2	3	4	1	2	3	4
1	34,08	8035	29,84	3566	50,28	37,23	57,97	65,83
2	50,71	100,16	45,20	29,48	65,55	50,09	60,18	69,47
3	63,62	85,05	39,77	30,40	50,45	41,14	60,09	59,08
4	56,38	66,48	42,90	29,31	48,80	44,99	55,66	49,87
5	52,21	46,00	35,57	27,17	41,77	45,46	48,76	37,03
6	40,39	93,62	37,06	22,55	36,01	27,03	27,63	44,99
7	45,19	85,02	25,89	25,50	40,55	48,07	47,19	74,51
8	59,60	79,76	31,23	48,86	44,72	50,94	43,87	51,41
9	54,84	65,69	37,71	51,56	33,07	45,78	48,57	40,32
10	61,46	55,55	36,56	25,61	31,17	42,58	50,55	40,91
11	56,70	85,59	26,79	36,92	36,20	41,73	38,93	44,23
12	54,37	87,13	26,58	26,91	32,45	43,51	43,20	70,20
13	57,30	79,17	34,02	54,40	39,12	39,36	43,91	64,18
14	51,14	77,06	33,80	46,94	30,54	39,29	53,28	48,93
15	44,63	63,27	36,90	26,82	33,57	42,69	49,12	42,23

Source: Authors

The Bland-Altman method was used to plot the differences in the average mean temporal amplitude values of the acquired sEMG signal using both types of electrodes (Figure 7). The limits of agreement (-6,7164 mV, 49,2496 mV) exhibited 95% (57/60) of difference scores. The mean difference (bias) in the measurements of the sEMG-DRY and the sEMG-GEL electrodes was $\overline{d} = 21,2666\,\text{mV}$. The SD of the differences was 13,9915 mV, and the width of 95% of the limits of agreement was 55,966 mV.

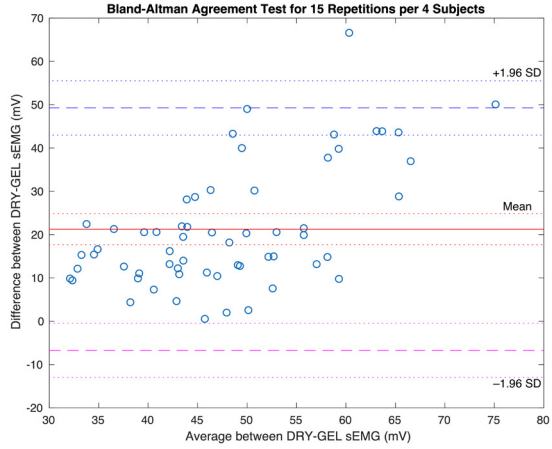

Figure 7. Bland-Altman plot of agreement. The differences between the sEMG-DRY and the sEMG-GEL electrodes are drawn against the mean of the paired measurements. For a normal distribution, at least 95% of the data are expected to land within the limits of agreement.
Source: Authors

The values of difference were normally distributed (Gaussian), showing approximately 73% of the differences (44/60) within one SD of the mean. 95% of the differences landed within two SDs (57/60) in the plot, and 98,3% were within three SDs (59/60).

The 95% CI was calculated by finding the point of t-distribution, with n-1 degrees of freedom, adding/subtracting the t standard error. For the amplitude data corresponding to Equations (4) and (5), the SD was 13,9915 mV, the SEM was 1,8063 mV, and the SELA was 3,1286 mV. For the 95% CI in Equation (6), there were 59 degrees of freedom and t = 2,0010. Hence, the 95% CI for the bias ranged from 17,6522 to 24,8810 mV. The 95% CI for the lower limit (LL) of agreement in Equation (7) was from -12,9767 to -0,4560 mV. For the upper limit (UL) of agreement, as per Equation (8), the 95% CI ranged from 42,9893 to 55,5099 mV.

FELT evaluation 1: anatomical array

The FELT anatomical array was designed and manufactured using dry electrodes and an anthropometrical textile sleeve. The FELT is a wearable APA using a sleeve placed on the forearm. It houses eight bipolar channels of sEMG electrodes to acquire hand movement signals with the Shimmer3 system. The average positions of the *individual templates* were used to determine the final anatomical positioning, which resulted in the proposal of a *general template*. This development translated into an easy-to-place APA fixed on a textile sleeve, able to hold eight pairs of sEMG-DRY. The original design, along with several views of the manufactured FELT, is shown in Figure 8.

There is an elastic band at the top of the sleeve, which contains the reference electrode that is placed at the olecranon (Figure 5a). The FELT was designed using anthropometric measurements taken from 17 abled-body volunteers with heights ranging from 1,50 to 1,90 m and weights from 50 to 110 kg.

The fabric used is soft, antibacterial, stretchable, and breathable, providing numerous benefits. These advantages make the sleeve comfortable to wear and help to secure the electrodes in place on the forearm. According to Kusche *et al*. (2019), dry electrode measurements should ensure that the electrode has enough contact force and that it works within the desired frequency range. The less the electrodes move, the fewer artifacts there will be.

The FELT anatomical array is designed to acquire sEMG signals closer to the main source for each movement. To this effect, it incorporates eight bipolar channels of dry electrodes and a reference. When a hand movement is performed, the FELT moves with the forearm and the hand, without restricting the range of movement. Although the FELT is wired, the use of Shimmer3 connected via Bluetooth to a computer transforms the FELT into a wearable, portable device that can have applications not only for control, but also for evaluations during various actions.

FELT evaluation 2: signal acquisition and data processing

The proper placement of the FELT is the difference between useful and useless signals. A FELT positioning protocol was designed and followed each time the sleeve was used in a trial. Placing the FELT was a straightforward process, which can be seen in Figure 3. Once the sleeve is on the forearm, the most important step is to ensure proper positioning by aligning the seams of the sleeve with two anatomical points: the ulnar fossa (the middle point of the elbow crease) and the middle point of the flexor retinaculum (a transversal ligament located across the wrist).

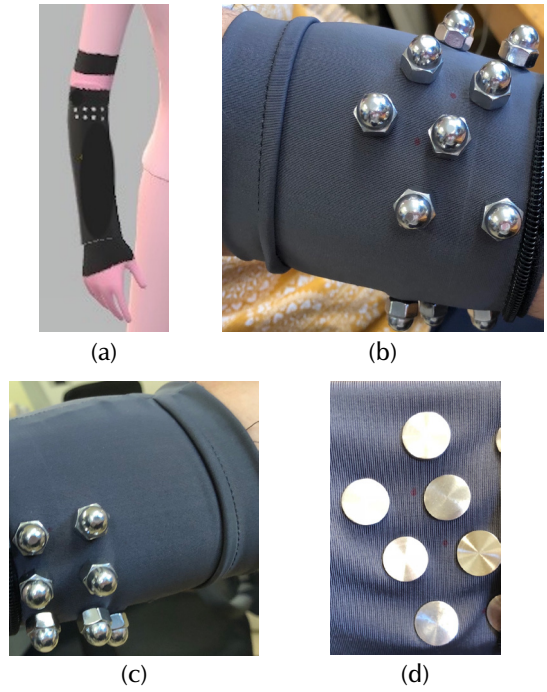

Figure 8. FELT Prototype. A) Simulation of the FELT, b) top view of the FELT prototype, c) bottom view of the FELT prototype, and d) internal view of FELT prototype, showing the inner side of the sEMG-DRY electrodes in contact with the skin.
Source: Authors

After placement, the sEMG signals were acquired. Two bipolar channels were recorded for hand opening and power grasp movements. Hand opening and power grasping are antagonist movements and activate antagonist muscles (brachioradialis and finger flexors *vs.* fingers extensors, which correspond to channels 1 and 5 of the FELT).

Over ten sessions, the main contribution of hand opening movements can be seen in channel 1 (mean absolute value or MAV of 80,42 ± 6,70 mV), while Channel 5 shows lower amplitudes (MAV of 18,69 ± 0,79 mV). For power grasping, the behavior is quite different, as channels 1 and 5 activate, albeit with lower amplitude values (channel 1: MAV of 39,93 ± 4,29 mV; channel 2: MAV of 32,38 ± 3,48 mV). The

variations observed over ten sessions are measured for each channel and movement. These results are shown in Table 4. The maximum amplitude variation, occurring in channel 1, showed a 24,81% change in the MAV of the sEMG signal between sessions 8 and 9 for hand opening movements.

Five sessions were conducted, and sEMG signals were acquired using the FELT and Shimmer3 with eight recording channels for six hand movements: hand opening, power grasp, fine pinch, supination, pronation, and rest. Then, the parameters were calculated for each movement and were used to build the features vectors to feed the ANN. To this effect, the Equations in Table 2 were used.

Table 4. Results obtained for the amplitude variations over 10 sessions of sEMG signal acquisition using the FELT for six hand movements. Channel 1 and 5 amplitude variations between contiguous sessions are presented, featuring the maximum variation value.

Session No.	Movement			
	Hand Opening		Power Grasp	
	Channel 1 Amplitude Variation [%]	Channel 5 Amplitude Variation [%]	Channel 1 Amplitude Variation [%]	Channel 5 Amplitude Variation [%]
1	-	-	-	-
2	11,17	8,55	1,69	3,04
3	3,54	6,29	1,94	9,18
4	14,73	2,78	13,73	11,59
5	7,17	8,36	5,92	6,56
6	4,91	3,88	2,56	0,31
7	7,89	6,62	1,54	4,04
8	1,37	2,03	5,46	2,64
9	24,81	10,22	17,92	14,09
10	5,24	6,71	9,37	9,44
MAXIMUM VARIATION VALUE (%)	**24,81**	**10,22**	**17,92**	**14,09**

Source: Authors

A six-class feed-forward ANN was used, with Bayesian regularization as the transfer function ('trainbr'). Bayesian regularization is a technique that introduces prior knowledge into the learning process to prevent overfitting and improve the network's generalization ability. This type of model is used for pattern recognition when there is a low number of repetitions and large features vectors. The ANN had six outputs and 56 inputs set up according to the previously calculated parameters. Data division was randomized. Performance was calculated through the sum squared error function. The vectors of parameters used for validation were not shared with the training and testing process.

sEMG signals are stochastic and their behavior depends on several factors such as the number of repetitions in a session, the lactate released the day before, and fatigue during the session or from days before the trial. A way to customize the algorithms to fit every individual is to build a new classifier in each session. For the five sessions conducted, the average accuracy was 97,86 ± 0,58%. This six-class classifier has a sensitivity of 0,9787, and a specificity of 0,9955. These values are shown in Table 5.

Table 5. Results obtained regarding classifier accuracy over five sEMG signal acquisition sessions

Session No.	Classifier Efficiency (%)	Classifier Error (%)
1	97,8	2,2
2	98,5	1,5
3	98,4	1,6
4	97,4	2,6
5	97,2	2,8
Mean ± SD	**97,86 ± 0,58**	**2,14 ± 0,58**

Source: Authors

Classifier efficiency values showed that the FELT allowed for the acquisition of sEMG signals containing the characteristic patterns of muscles to differentiate between the six hand movements. These are useful evaluations, since the algorithms adjust to the characteristic features of the trial subject during the session. This type of flexibility works in favor of the subject because they do not have to force-fit the system; the system fits them. Thus, if the session is longer, the system may readjust, or the subjects could take a break, take out the FELT, and come back later, position the FELT, re-calibrate the classifier, and have a second session. No extra electrodes are wasted, and no skin irritation caused by taking the electrodes off and on will occur.

Regarding other works that classify hand movements based on sEMG signals and pattern recognition using neural network approaches, Kang *et al*. (2023) present a hand gesture recognition system using a binarized neural network, reporting a 95,4% classification accuracy for four gestures from a single sEMG channel. Lee *et al*. (2023) report 97% accuracy while using a stretchable array of eight pairs of fabric-based sEMG electrodes, and Tepe and Demir (2022) report mean accuracies of around 95,83% while using the commercial Myo band sEMG acquisition system.

The Myo armband is probably the most used device for prosthetic control in research (Abduo and Galster, 2015; Chen *et al*., 2020; Morais *et al*., 2016; Visconti *et al*., 2018; Yakob *et al*., 2021). It was originally designed to be used by the public as an everyday-life control device. It has a very sturdy design, and the circumference adapts to different arm thicknesses. It is calibrated at the beginning of each use, meaning that it adapts the algorithm to the sEMG signals acquired, so it can be re-calibrated as needed when the sEMG signals change. The embedded acquisition system has a limited frequency spectrum (0-100 Hz), but the full sEMG spectrum goes up to 500 Hz (Pizzolato *et al*., 2017). Moreover, the battery time of this device is limited.

Other acquisition configurations have been tested for recording sEMG signals, such as the Otto Bock 13 E200 and the Delsys Trigno setups (Pizzolato *et al*., 2017). Both systems have pre-positioned dry electrodes. In the case of the Delsys Trigno, the placing sites must be determined by

the user. The Otto Bock system has an equidistant array of electrodes around the circumference of the forearm.

The proposed FELT array has an anatomical design that positions the dry electrodes closer to the source of different sEMG signal patterns. After signal processing, this allows an ANN to classify the signal with high accuracy.

Our device can be used with any acquisition system, and one can use as many electrodes as needed. Some drawbacks of the FELT array include issues such as the fact that it is wired to the acquisition system and, although it can be detached, processing must be conducted in order to enhance the sEMG signal, as it has a noisier-than-desirable raw signal.

As described by Al-Ayyad *et al*. (2023), the use of sEMG signals is migrating from prosthetic control towards use in rehabilitation training and physiological tracking. sEMG signal applications are moving towards anticipating trajectories for one arm based on the movement of the other.

Future work regarding this development will focus on the implementation of a small detachable acquisition system aimed at transforming the FELT into a wearable that can be used in different applications. An important one has to do with virtual/augmented reality (VR/AR) interfaces and serious games (Toledo-Peral *et al*., 2022). We believe that the proposal of arrays such as the one in this article may provide a better starting point for these developments, and that VR/AR applications will certainly benefit from sEMG signals as a control for present and future movements, in addition to being an evaluation stage for previous ones, thus closing the biofeedback loop.

The FELT anatomical array is a proposal aimed at embracing an organic design that is focused on the user and tries to harness bio-signals with less intervention during movements, hoping for better results in clinical applications, mainly in the field of rehabilitation.

As with most developments, this design is subject to limitations, which include the low number of test subjects. In addition, not all subjects may fit the textile sleeve; a larger or smaller one may be needed. This also limits the variety of sEMG signals acquired. It is necessary to include a larger and more varied demographic for both sleeve design and signal acquisition, which might imply changes in the classifier algorithm. Moreover, there is always room for improvement in the design of the electrodes.

Conclusions

An anatomical positioning forearm dry electrode array fixed on a textile sleeve (called *FELT*) was designed and built to acquire eight bipolar channels of sEMG signals from hand movements. The fabric has antibacterial and breathability properties that allow subjects to be comfortable while ensuring that the dry electrodes have a tight fit to the skin in order to avoid movement artefacts, which is crucial in dynamic measurements. The anatomical design is based on anthropometrical measures, which allows the FELT to pick up sEMG signals closer to the ventral area of the muscles which corresponds to the movement performed, thus improving signal quality as well as the sleeve's fit around the forearm.

Even though the sEMG-DRY electrodes, as any dry electrode, yield a noisier signal than that of sEMG-GEL electrodes, the digital signal processing performed, which is based on the DWT technique, allows making the signals comparable to those acquired with the pre-gelled electrodes. We proved this by means of the Bland-Altman agreement assessment, which showed a 95% agreement between both signals. This means that the signals from the sEMG-DRY electrodes can be used with the same confidence as those from the others.

Still, this might sound like a contradiction. Why should we substitute pre-gelled electrodes for noisier dry electrodes and have to go through a different type of processing to get a similar result? The answer is simple. It is complicated to place that many electrodes repeatedly for long periods of time without skin irritation, l*et al*one place them always at the same location, and it is even more difficult to find the correct anatomical positions without prior knowledge. These results show that the FELT is usable for hand movement signal acquisition.

Another important aspect to consider is placement. A positioning protocol was developed to serve as a guideline to properly place the FELT on the forearm, and, even though the protocol is based on anatomical markers, the procedure is straightforward. This is seen in Figure 3. It is also important to ensure repeatability, and, in this case, the difficulty was to find a parameter to evaluate and help calibrate the changes between sessions. To this effect, we calculated the MAV of sEMG signals from the antagonist muscles for hand opening and power grasp movements (brachioradialis and finger flexors *vs.* finger extensors, corresponding to channels 1 and 5). We then calculated the variations between each session, and found the maximum value to be 24,81%. The variations in the positioning of the FELT could thus be quantified using the same signals acquired in the trials. On top of that, as shown in the *Results and discussion* section (*FELT evaluation 2: signal acquisition and data processing*), we built a classifier that recalibrates for each session and proved to have an efficiency of over 97,86 ± 0,58% in differentiating between six hand movements.

Acknowledgements

Funding was received by the National Science and Technology Council (CONACYT) of Mexico, through the project CONACYT-SALUD-2016-01-272983. We also appreciate the funding for the development of this work through ERAnet-EMHE 200022, CYTED-DITECROD-218RT0545, and Proyecto IV-8 call Amexcid-Auci 2018-2020.

The authors would like to thank Gerardo Hernández-Nava, José Antonio Mejía-Licona, and Othón Benítez-Keller for their technical support during the experiments performed, as well as Dr. Jaime H. Guadarrama-Becerril for his input in helping to establish the anthropometrical bases to develop the textile sleeve.

Author contributions

Cinthya Lourdes Toledo-Peral: conceptualization, visualization, methodology, validation, formal analysis, investigation, writing – original draft, review, and editing. Ana Isabel Martín-Vignon-Whaley: methodology, formal analysis, investigation, writing – original draft, review, and editing. Jorge A. Mercado-Gutiérrez: methodology, writing – review & editing. Arturo Vera-Hernández: supervision, funding acquisition, writing – review and editing. Lorenzo Leija-Salas: supervision, project administration, funding acquisition, writing – review and editing. Josefina Gutiérrez-Martinez: supervision, project administration, writing – review and editing.

Conflicts of interest

The authors declare that they have no conflict of interest.

Data availability

The data are protected by the Institutional Ethics Board, and, in case of need, they should be requested through them.

CRediT author statement

All authors: conceptualization, methodology, software, validation, formal analysis, investigation, writing (original draft, writing, review, and editing), data curation.

References

Abduo, M., and Galster, M. (2015). *Myo gesture control armband for medical* applications [Bachelor thesis, University of Canterbury]. http://hdl.handle.net/10092/14449

Al-Ayyad, M., Owida, H. A., De Fazio, R., Al-Naami, B., and Visconti, P. (2023). Electromyography monitoring systems in rehabilitation: A review of clinical applications, wearable devices and signal acquisition methodologies, *Electronics (Switzerland)*, *12*(7), 1520. https://doi.org/10.3390/electronics12071520

Albulbul, A. (2016). Evaluating major electrode types for idle biological signal measurements for modern medical technology. *Bioengineering*, *3*(3), 20. https://doi.org/10.3390/bioengineering3030020

Barbero, M., Merletti, R., and Rainoldi, A. (2012a). *Atlas of muscle innervation zones*. Springer. https://doi.org/10.1007/978-88-470-2463-2

Barbero, M., Merletti, R., and Rainoldi, A. (2012b). EMG imaging: Geometry and anatomy of the electrode-muscle system. In Springer (Eds.), *Atlas of Muscle Innervation Zones* (pp. 39-47). Springer. https://doi.org/10.1007/978-88-470-2463-2_4

Besomi, M., Hodges, P. W., van Dieën, J., Carson, R. G., Clancy, E. A., Disselhorst-Klug, C., Holobar, A., Hug, F., Kiernan, M. C., Lowery, M., McGill, K., Merletti, R., Perreault, E., Søgaard, K., Tucker, K., Besier, T., Enoka, R., Falla, D., Farina, D., ... Wrigley, T. (2019). Consensus for experimental design in electromyography (CEDE) project: Electrode selection matrix. *Journal of Electromyography and Kinesiology*, *48*, 128-144. https://doi.org/10.1016/j.jelekin.2019.07.008

Biga, L. M., Dawson, S., Harwell, A., Hopkins, R., Kaufmann, J., LeMaster, M., Matern, P., Morrison-Graham, K., Quick, D., and Runyeon, J. (n.d.). *Explain the organization of muscle fascicles and their role in generating force*. https://open.oregonstate.education/aandp/chapter/11-2-explain-the-organization-of-muscle-fascicles-and-their-role-in-generating-force/#:~:text=When%20a%20group%20of%20muscle,the%20muscle's%20range%20of%20motion

Bland, J. M., and Altman, D. G. (1986). Statistical methods for assessing agreement between two methods of clinical measurement. *Lancet*, *1*(8476), 307-310.

Chen, L., Fu, J., Wu, Y., Li, H., and Zheng, B. (2020). Hand gesture recognition using compact CNN via surface electromyography signals. *Sensors*, *20*(3), 672. https://doi.org/10.3390/s20030672

Chi, Y. M., Jung, T.-P., and Cauwenberghs, G. (2010). Dry-contact and noncontact biopotential electrodes: Methodological review. *IEEE Reviews in Biomedical Engineering*, *3*, 106-119. https://doi.org/10.1109/RBME.2010.2084078

Dai, C., Zhu, Z., Martinez-Luna, C., Hunt, T. R., Farrell, T. R., and Clancy, E. A. (2019). Two degrees of freedom, dynamic, hand-wrist EMG-force using a minimum number of electrodes. *Journal of Electromyography and Kinesiology*, *47*, 10-18. https://doi.org/10.1016/j.jelekin.2019.04.003

Gan, Y., Vauche, R., Pons, J. F., and Rahajandraibe, W. (2019). *Dry electrode materials for electrocardiographic monitoring* [Conference presentation]. 2018 25th IEEE International Conference on Electronics Circuits and Systems, Bourdeaux, France. https://doi.org/10.1109/ICECS.2018.8617992

Garcia, G. A., Zaccone, F., Ruff, R., Micera, S., Hoffmann, K.-P., and Dario, P. (2007). *Characterization of a new type of dry electrodes for long-term recordings of surface-electromyogram* [Conference presentation]. 2007 IEEE 10th International Conference on Rehabilitation Robotics, Noordwijk, Netherlands. https://doi.org/10.1109/ICORR.2007.4428523

Ghoshdastider, U., Lange, C., Viga, R., and Grabmaier, A. (2012). *A modular and wireless exg signal acquisition system with a dense array of dry electrodes* [Conference presentation]. IEEE Sensors 2012, Taipei, Taiwan. https://doi.org/10.1109/ICSENS.2012.6411473

Guo, L., Sandsjö, L., Ortiz-Catalan, M., and Skrifvars, M. (2020). Systematic review of textile-based electrodes for long-term and continuous surface electromyography recording. *Textile Research Journal*, *90*(2), 227-244. https://doi.org/10.1177/0040517519858768

Guzmán, R. A., Silvestre, R. A., and Arriagada, D. A. (2011). Biceps brachii muscle innervation zone location in healthy subjects using high-density surface electromyography. *International Journal of Morphology*, *29*(2), 347-352. https://doi.org/10.4067/s0717-95022011000200007

Hall, J. E. (2011). *Guyton & Hall: tratado de fisiología medica*. Elsevier.

Hermens, H. J., Freriks, B., Disselhorst-Klug, C., and Rau, G. (2000). Development of recommendations for SEMG sensors and sensor placement procedures. *Journal of Electromyography and Kinesiology: Official Journal of the International Society of Electrophysiological Kinesiology*, *10*(5), 361-374. https://doi.org/10.1016/s1050-6411(00)00027-4

Kang, S., Kim, H., Park, C., Sim, Y., Lee, S., and Jung, Y. (2023). sEMG-based hand gesture recognition using binarized neural network. *Sensors*, *23*(3), 1436. https://doi.org/10.3390/s23031436

Kapelner, T., Jiang, N., Holobar, A., Vujaklija, I., Roche, A. D., Farina, D., and Aszmann, O. C. (2016). Motor unit characteristics after targeted muscle reinnervation. *PLoS ONE*, *11*(2), 0149772. https://doi.org/10.1371/journal.pone.0149772

Kusche, R., Kaufmann, S., and Ryschka, M. (2019). Dry electrodes for bioimpedance measurements - Design, characterization and comparison. *Biomedical Physics and Engineering Express*, *5*(1), 015001. https://doi.org/10.1088/2057-1976/aaea59

Lee, H., Lee, S., Kim, J., Jung, H., Yoon, K. J., Gandla, S., Park, H., and Kim, S. (2023). Stretchable array electromyography sensor with graph neural network for static and dynamic gestures recognition system. *Npj Flexible Electronics*, *7*(1), 20. https://doi.org/10.1038/s41528-023-00246-3

Liu, J. (2015). Adaptive myoelectric pattern recognition toward improved multifunctional prosthesis control. *Medical Engineering and Physics*, *37*(4), 424-430. https://doi.org/10.1016/j.medengphy.2015.02.005

Losier, Y., Clawson, W., Scheme, E., Englehart, K., Kyberd, P., and Hudgins, B. (2011). *An overview of the UNB hand system* [Conference presentation]. MyoElectric Controls/Powered Prosthetics Symposium Fredericton, NB, Canada.

Martin, A. I., Toledo, C., Mercado, J. A., Vera, A., Leija, L., and Gutierrez, J. (2018). *Evaluation of dry electrodes for sEMG recording* [Conference presentation]. 2018 Global Medical Engineering Physics Exchanges/Pan American Health Care Exchanges (GMEPE/PAHCE), Porto, Portugal. https://doi.org/10.1109/GMEPE-PAHCE.2018.8400758

Merletti, R., and Farina, D. (Eds.) (2016). *Surface electromyography physiology, engineering, and applications*. John Wiley & Sons.

Meziane, N., Webster, J. G., Attari, M., and Nimunkar, A. J. (2013). Dry electrodes for electrocardiography. *Physiological Measurement*, *34*(9), R47-R69. https://doi.org/10.1088/0967-3334/34/9/R47

Mitchell, B., & Whited, L. (2019). *Anatomy, shoulder and upper limb, forearm muscles*. https://www.ncbi.nlm.nih.gov/books/NBK536975/

Moin, A., Zhou, A., Rahimi, A., Benatti, S., Menon, A., Tamakloe, S., Ting, J., Yamamoto, N., Khan, Y., Burghardt, F., Benini, L., Arias, A. C., and Rabaey, J. M. (2018). *An EMG gesture recognition system with flexible high-density sensors and brain-inspired high-dimensional classifier* [Conference presentation]. IEEE International Symposium on Circuits and Systems, Florence, Italy. https://doi.org/10.1109/ISCAS.2018.8351613

Morais, G. D., Neves, L. C., Masiero, A. A., and Castro, M. C. F. (2016). *Application of Myo Armband System to control a robot interface* [Conference presentation]. BIOSIGNALS 2016 - 9th International Conference on Bio-Inspired Systems and Signal Processing, Rome, Italy. https://doi.org/10.5220/0005706302270231

Niu, X., Gao, X., Liu, Y., and Liu, H. (2021). Surface bioelectric dry Electrodes: A review. *Measurement: Journal of the International Measurement Confederation*, *183*, 109774. https://doi.org/10.1016/j.measurement.2021.109774

Palumbo, A., Vizza, P., Calabrese, B., and Ielpo, N. (2021). Biopotential signal monitoring systems in rehabilitation: A review. *Sensors, 21*(21), 7172. https://doi.org/10.3390/s21217172

Peng, Y., He, J., Yao, B., Li, S., Zhou, P., and Zhang, Y. (2016). Motor unit number estimation based on high-density surface electromyography decomposition. *Clinical Neurophysiology*, *127*(9), 3059-3065. https://doi.org/10.1016/j.clinph.2016.06.014

Phinyomark, A., Quaine, F., Charbonnier, S., Serviere, C., Tarpin-Bernard, F., and Laurillau, Y. (2013). EMG feature evaluation for improving myoelectric pattern recognition robustness. *Expert Systems with Applications*, *40*(12), 4832-4840. https://doi.org/10.1016/j.eswa.2013.02.023

Phinyomark, A., Quaine, F., Charbonnier, S., Serviere, C., Tarpin-Bernard, F., and Laurillau, Y. (2014). Feature extraction of the first difference of EMG time series for EMG pattern recognition. *Computer Methods and Programs in Biomedicine*, *117*(2), 247-256. https://doi.org/10.1016/j.cmpb.2014.06.013

Pizzolato, S., Tagliapietra, L., Cognolato, M., Reggiani, M., Müller, H., and Atzori, M. (2017). Comparison of six electromyography acquisition setups on hand movement classification tasks. *PLoS ONE*, *12*(10), 0186132. https://doi.org/10.1371/journal.pone.0186132

Puurtinen, M. M., Komulainen, S. M., Kauppinen, P. K., Malmivuo, J. A. V., and Hyttinen, J. A. K. (2006). *Measurement of noise and impedance of dry and wet textile electrodes, and textile electrodes with hydrogel* [Conference presentation]. 2006 International Conference of the IEEE Engineering in Medicine and Biology Society, New York, NY, USA. https://doi.org/10.1109/IEMBS.2006.260155

Reategui, J., and Callupe, R. (2017). *Surface EMG multichannel array using active dry sensors for forearm signal extraction* [Conference presentation]. 2017 IEEE 24th International Congress on Electronics, Electrical Engineering and Computing, Cusco, Peru. https://doi.org/10.1109/INTERCON.2017.8079699

"Recommendations for the practice of clinical neurophysiology: Guidelines of the International Federation of Clinical Neurophysiology" (1999). *Electroencephalography and Clinical Neurophysiology*, *52*(supp.), 1-304.

Rodrigues, M. S., Fiedler, P., Küchler, N., Domingues, R. P., Lopes, C., Borges, J., Haueisen, J., and Vaz, F. (2020). Dry

electrodes for surface electromyography based on architectured titanium thin films. *Materials*, *13*(9), 2135. https://doi.org/10.3390/ma13092135

Rojas-Martínez, M., Mañanas, M. A., Alonso, J. F., and Merletti, R. (2013). Identification of isometric contractions based on High Density EMG maps. *Journal of Electromyography and Kinesiology*, *23*(1), 33-42. https://doi.org/10.1016/j.jelekin.2012.06.009

Rui Ma, Dae-Hyeong Kim, McCormick, M., Coleman, T., and Rogers, J. (2010). *A stretchable electrode array for non-invasive, skin-mounted measurement of electrocardiography (ECG), electromyography (EMG) and electroencephalography (EEG)* [Conference presentation]. 2010 Annual International Conference of the IEEE Engineering in Medicine and Biology, Buenos Aires, Argentina. https://doi.org/10.1109/IEMBS.2010.5627315

Ruvalcaba, A., Altamirano, A., Toledo, C., Munoz, R., Vera, A., and Leija, L. (2016). Design and measurement of the standards of a miniaturized sEMG acquisition system with dry electrodes integrated [Conference presentation]. 2015 International Conference on Mechatronics, Electronics, and Automotive Engineering, Cuernavaca, Mexico. https://doi.org/10.1109/ICMEAE.2015.34

Ruvalcaba, A., Muñoz, R., Vera, A., and Leija, L. (2017a). Design and test of a dry electrode array implemented on wearable sEMG acquisition sleeve for long term monitoring [Conference presentation]. Pan American Health Care Exchanges, *PAHCE*, *2017-March*. https://doi.org/10.1109/GMEPE-PAHCE.2017.7972111

Srinivasa, M. G., and Pandian, P. S. (2017). *Dry electrodes for bio-potential measurement in wearable systems* [Conference presentation]. 2017 2nd IEEE International Conference on Recent Trends in Electronics, Information & Communication Technology (RTEICT), Bangalore, India. https://doi.org/10.1109/RTEICT.2017.8256600

Tepe, C., and Demir, M. C. (2022). Real-time classification of EMG Myo Armband data using support vector machine. *IRBM*, *43*(4), 300-308. https://doi.org/10.1016/j.irbm.2022.06.001

Toledo, C., Flores, E., Mercado, J., Castellanos, P., and Gutiérrez, J. (2018, September 26). *Multiclass sEMG signal processing and classification for upper-limb FES-NP control* [Conference presentation]. Annual Conference of the German Society for Biomedical Engineering, Aachen, Germany.

Toledo-Peral, C. L., Gutiérrez-Martínez, J., Mercado-Gutiérrez, J. A., Martín-Vignon-Whaley, A. I., Vera-Hernández, A., and Leija-Salas, L. (2018). sEMG Signal Acquisition Strategy towards Hand FES Control. *Journal of Healthcare Engineering*, *2018*, 2350834. https://doi.org/10.1155/2018/2350834

Toledo-Peral, C. L., Vega-Martínez, G., Mercado-Gutiérrez, J. A., Rodríguez-Reyes, G., Vera-Hernández, A., Leija-Salas, L., and Gutiérrez-Martínez, J. (2022). Virtual/augmented reality for rehabilitation applications using electromyography as control/biofeedback: Systematic literature review. *Electronics*, *11*(14), 2271. https://doi.org/10.3390/electronics11142271

Topalović, I., Graovac, S., and Popović, D. B. (2019). EMG map image processing for recognition of fingers movement. *Journal of Electromyography and Kinesiology*, *49*, 102364. https://doi.org/10.1016/j.jelekin.2019.102364

Urbanek, H., and van der Smagt, P. (2016). IEMG: Imaging electromyography. *Journal of Electromyography and Kinesiology*, *27*, 1-9. https://doi.org/10.1016/j.jelekin.2016.01.001

Visconti, P., Gaetani, F., Zappatore, G. A., and Primiceri, P. (2018). Technical features and functionalities of Myo armband: An overview on related literature and advanced applications of myoelectric armbands mainly focused on arm prostheses. *International Journal on Smart Sensing and Intelligent Systems*, *11*(1), 1-25. https://doi.org/10.21307/ijssis-2018-005

Vojtech, L., Bortel, R., Neruda, M., and Kozak, M. (2013). Wearable textile electrodes for ECG measurement. *Advances in Electrical and Electronic Engineering*, *11*(5), 410-414. https://doi.org/10.15598/aeee.v11i5.889

Xie, L. Yang, G., Xu, L., Seoane, F., Chen, Q., and Zheng, L. (2013). *Characterization of dry biopotential electrodes* [Conference presentation]. 2013 35th Annual International Conference of the IEEE Engineering in Medicine and Biology Society (EMBC), Osaka, Japan. https://doi.org/10.1109/EMBC.2013.6609791

Yakob, M. Y. bin, Baharuddin, M. Z. bin, Khairudin, A. R. M., and Karim, M. H. B. A. (2021). Telecontrol of prosthetic robot hand using Myo Armband [Conference presentation]. 2021 IEEE International Conference on Automatic Control and Intelligent Systems, I2CACIS 2021, Shah Alam, Malaysia. https://doi.org/10.1109/I2CACIS52118.2021.9495919

Young, A. J., Hargrove, L. J., and Kuiken, T. A. (2011). The Effects of Electrode Size and Orientation on the Sensitivity of Myoelectric Pattern Recognition Systems to Electrode Shift. *IEEE Transactions on Biomedical Engineering*, *58*(9), 2537-2544. https://doi.org/10.1109/TBME.2011.2159216